UNIVERSITY OF CALIFORNIA SAN DIEGO

Evaluating Patient-Specific Computational Models of Dyssynchronous Heart Failure

A Thesis submitted in partial satisfaction of the requirements for the degree
Master of Science

in

Bioengineering

by

Michael Russell Young

Committee in charge:

Professor Andrew D. McCulloch, Chair
Professor David Krummen
Professor Jeffrey H. Omens

2018

The Thesis of Michael Russell Young is approved, and it is acceptable in quality and form for publication on microfilm and electronically:

_____

_____

_____
Chair

University of California San Diego

2018

DEDICATION

I dedicate this thesis to my family. Thank you for encouraging me to reach for bigger and bigger goals, even when they directly inconvenience you. Thank you for your persistent belief in me. To my dad, thank you for encouraging my constant questioning while we worked on cars. It taught me a lot about how machines work and why things are designed the way they are. To my mom, thank you for the unconditional support. It probably is not easy to assure your son that he should move as far away as possible in the contiguous United States, but I really needed your assurance. To my brother, thanks for teaching me to do my research before I make an argument. One really must have a lot of evidence to change your mind.

TABLE OF CONTENTS

Signature Page iii

Dedication iv

Table of Contents v

List of Figures viii

List of Tables ix

List of Abbreviations x

Acknowledgements xii

Abstract of the Thesis xiii

Chapter 1 : Background 1

1.1 Cardiac Anatomy and Physiology 1

1.2 Dyssynchronous Heart Failure 2

1.3 Cardiac Resynchronization Therapy 3

1.3.1 Successes 3

1.3.2 Nonresponders 6

1.3.3 Hyper-responders 8

1.4 Dyssynchrony Metrics 9

1.4.1 QRS Area 9

1.4.2 Circumferential Uniformity Ratio Estimate 9

1.4.3 Internal Stretch Fraction 10

1.4.4 Coefficient of Variation of Regional Work 10

1.4.5 Volume Fraction of Negative Work 11

1.5 Finite Element Models for Cardiac Electromechanical Simulations 11

1.5.1 Cardiac Geometry 12
1.5.1 Activation Pattern 12
1.5.2 Constitutive Models 12
1.5.3 Active Tension Models 13
1.5.4 Circulatory Model 14
1.6 Specific Aims 14
Chapter 2 : Methods 16
2.1 Patient Data Collection 16
2.2 Mesh Generation 17
2.3 Fiber Fitting 18
2.4 Electrical Activation Maps 19
2.5 Constitutive Model 20
2.6 Unloading Algorithm 21
2.7 Active model 21
2.8 Circulation Model 22
2.9 Full Beat Finite Elements Simulations 23
2.10 Dyssynchrony Metrics 23
Chapter 3 : Results 24
3.1 Model Comparison 24
3.1.1 Comparison with Patient Data 24
3.1.2 Comparison of Metrics 28
3.2 Sensitivity Analysis 30
3.2.1 Effects of Using Average Input Parameters 30

3.2.2 Identification of Important Global Features 31

Chapter 4 : Discussion 34

4.1 Simulation Findings 34

4.2 Limitations 36

4.3 Future Studies 37

References 38

LIST OF FIGURES

Figure 2.1: (A) Segmentation of CT imaging data. (B) Smoothed surfaces representing the LV endocardium (red) the RV endocardium (blue) and the epicardium (yellow). (C) 209-node template fit to the smoothed surfaces. (D) Finite element mesh after cubic splines were created in prolate spheroidal coordinates. 18

Figure 2.2: (A) Close up on an element, showing the transmural variation in fiber angle. (B) Showing spatial variation of fiber angle on the LV free wall. 19

Figure 2.3: (A) An example electrophysiology finite elements mesh. This mesh would be subdivided for simulations. (B) An example of an LBBB activation map. Red is early activated, and blue is late activated. 20

Figure 3.1: Comparing the two cohorts and the fitting of the data. The red is the new cohort and the black is the previous cohort. The lines connecting points from echo to model show the pairing of the data. The dots on the vertical lines are the mean, and the error bars are the standard deviation. 25

Figure 3.2: A view of the right ventricle of the model geometries. The outside is basal, and the middle is apical. (A) The earliest activated nodes for the previous cohort. There are fewer nodes than patients, because the same node was early activated for more than one patient. (B) The earliest activated nodes for the new cohort. 26

Figure 3.3: Comparison of dP/dt from the previous cohort in black and the new cohort in red. Notice the smaller range for the new cohort, because this was not fit to patient data. Instead, it correlates with the peak pressure. 27

Figure 3.4: (A) The comparison of EF. Because the new cohort was fit to the patient EF, it is much closer to the measured values. (B) The peak pressure was also fit in the new cohort instead of dP/dt max, so the models match the cuff peak pressure very well. .. 28

Figure 3.5: The left column shows the mean and variation of the metrics themselves. The right column shows the correlation with reverse remodeling. (A) New cohort (red) has less variation and is in general less dyssynchronous. (B) The VFLVNW vs. ESV reduction. A higher ESV reduction indicates a bigger response to CRT. 29

Figure 3.6: (A) Heatmap showing the nRMSD from the fully patient-specific model to the averaged parameter listed on the left. CA is the circulation model, ME is mechanical properties, CT is the geometry, and AT is the activation pattern. The bottom labels designate for which metric the nRMSD was calculated. 31

Figure 3.7: (A) The LVEDP from the fully patient-specific models plotted against the LVEDP from both the average circulation models and the average mechanics models. The line of best fit has the r^2 value and slope indicated in the heatmaps C and D. An r^2 value and slope of 1 indicates no change in the parameters. 32

LIST OF TABLES

Table 2.1: Summary of echocardiographic data retrieved prior to CRT device implant 16

Table 3.1: Results of correlating the residuals for the circulatory model. The four parameters that correlated best are shown. Notice how most have to do with ventricular filling via vein pressure or the atria …….…... 33

LIST OF ABBREVIATIONS

AUC	Area under curve
COVW	Coefficient of variation of work
CRT	Cardiac resynchronization therapy
CT	Computed tomography
CURE	Circumferential uniformity ratio estimate
DCM	Dilated cardiomyopathy
DHF	Dyssynchronous heart failure
dP/dt	Pressure rate of change
dV/dt	Volume rate of change
ECG	Electrocardiograph
EDP	End diastolic pressure
EF	Ejection fraction
ESV	End-systolic volume
ISF	Internal stretch fraction
IVSd	Interventricular septal thickness at end diastole
LBBB	Left bundle branch block
LVIDd	Left ventricular internal diameter at end diastole
LVPWd	Left ventricular posterior wall thickness
MR	Magnetic resonance
MR-MT	Magnetic resonance- myocardial tagging
NYHA	New York heart association

nRMSD	Normalized root mean squared deviation
ODE	Ordinary differential equation
PW	Pulsed wave
TDI	Tissue doppler imaging
VCG	Vectorcardiography
VFLVNW	Volume fraction of negative work in the left ventricle
VFNW	Volume fraction of negative work
VFSTNW	Volume fraction of negative work in the septum

ACKNOWLEDGEMENTS

I would like to acknowledge Dr. Andrew McCulloch and Dr. Jeff Omens for their guidance. I would like to acknowledge Dr. Kevin Vincent for his frequent advice and contribution to my own knowledge and the results of this thesis. I would like to acknowledge Dr. Chris Villongco and Dr. Adarsh Krishnamurthy for their advice, developing the methods that I used, creating the previous cohort of models, and running the sensitivity analysis.

ABSTRACT OF THE THESIS

Evaluating Patient-Specific Computational Models of Dyssynchronous Heart Failure

By

Michael Russell Young

Master of Science in Bioengineering

University of California San Diego, 2018

Professor Andrew D. McCulloch, Chair

Cardiac resynchronization therapy (CRT) is an effective treatment for dyssynchronous heart failure. Most patients perform better during clinical tests of cardiac function and may even have their hearts reverse remodel to a more normal state. As many as 30-40% of patients, however, do not respond. A focus of current research is identifying which patients will respond to CRT, though current clinical indications for CRT are based on dyssynchrony and heart failure and not on validated predictors of CRT response. In this thesis, five patient-specific computational models based on non-invasive data were developed and compared with

eight previous patient-specific models that were based on more detailed and invasive clinical information to test whether the dyssynchrony metrics from the original study were still predictive in the new group. Model properties such as the volume fraction of negative work (VFNW) and coefficient of variation of work (COVW), that had correlated with patient outcomes in the original cohort, did not correlate with reverse remodeling as measured by reduction in end-systolic volume in the new group. The sensitivity analysis showed that these quantities were sensitive to the parameters of ventricular filling mechanics that could not be included in patient-specific models based on non-invasive data. Non-invasive estimates of filling parameters are available, but their reliability has been questioned. We conclude that it is likely to be necessary to obtain invasive measurements of diastolic pressures for patient-specific models to predict CRT outcomes. However, these measurements are available by cardiac catheterization, which could be justified for CRT patients.

Chapter 1 : Background

1.1 Cardiac Anatomy and Physiology

The heart is a mechanical pump that generates pressure differentials to drive blood flow. The right atrium and ventricle deliver deoxygenated blood to the lungs via the pulmonary arteries. The left atrium and ventricle receive the blood from the lungs via the pulmonary veins and deliver oxygenated blood to the rest of the body through the systemic arteries. These two circulatory systems ensure that the various tissues of the body are provided with enough oxygen and nutrients to perform their functions.

The ventricles are the chambers that are responsible for generating the pressure differentials that cause the blood to flow through the arteries. Because the systemic blood vessels perfuse much more of the body, the left ventricle operates at higher pressures. The atria are responsible for collecting the blood from the veins and filling the ventricles. Uni-directional blood flow is maintained by four valves: the mitral valve, the tricuspid valve, the aortic valve, and the pulmonary valve. The mitral and tricuspid valves are between the left and right atria and ventricles, respectively, and are known as the atrioventricular valves. The aortic and pulmonary valves are between the systemic and pulmonary arteries and the ventricles and are known as the semilunar valves. All of the valves are pressure driven. They shut when the pressure gradient would act to push the blood in the reverse direction and open when the gradient is pushing the blood in the forward direction. All of the valves are in a similar region of the heart, known as the valve plane.

The muscular contractions in the heart are driven by electrical activation. In a healthy heart, the atria are activated first. The electrical impulse starts at the sinoatrial node and travels across the atria towards the valve plane. There is a short delay at the atrioventricular

node to allow the contracting atria to fill the ventricles, and then the electrical activation travels through the bundle of His to the left and right bundle branches to the left and right ventricles, which are activated synchronously to eject the blood. This synchronous activation is important for efficient contraction and blood ejection, and dyssynchronous activation can lead to a type of heart failure called dyssynchronous heart failure (DHF).

1.2 Dyssynchronous Heart Failure

When the conduction through the left bundle branch is lost, the electrical activation must travel through the muscular part of the heart, the myocardium, rather than the specialized conduction system. This is known as left bundle branch block (LBBB). LBBB results in a prolonged electrical activation and less efficient blood ejection. Of the people with heart failure, around half also have electrical conduction defects such as LBBB [1]. These electrical conduction defects can result in intraventricular dyssynchrony and/or interventricular dyssynchrony. Intraventricular dyssynchrony means that some parts of the ventricle are early activated, and some are late activated. Interventricular dyssynchrony means that the ventricles are activated at different times relative to each other.

One way to assess the impact of LBBB on the heart is to look at the length of the QRS complex on the electrocardiogram (ECG) and the direction of the vectorcardiogram (VCG) [2]. These can give clinicians a picture of how extensive the block is and how dyssynchronous the electrical activation is. LBBB typically causes an increased QRS duration and left axis deviation.

To assess the mechanical function of the dyssynchronous heart, echocardiography is typically used. Ejection fraction (EF) is used to determine how efficient the heart is at ejecting

blood. EF is normally greater than 55%; a low EF is one of the indicators that a patient is experiencing systolic heart failure. An increased end systolic volume (ESV) as measured by echocardiography is another indication that the patient has pathological remodeling leading to systolic dysfunction. Tissue doppler imaging (TDI) has been used to measure intraventricular dyssynchrony, by measuring myocardial motion in different areas [1] [3] [4]. To measure interventricular dyssynchrony, the difference between the beginning of the right and left ventricular flow velocity curves as measured by pulsed-wave (PW) Doppler has been used [1]. A therapy known as Cardiac Resynchronization Therapy (CRT) has been developed to correct the electromechanical dyssynchrony present in DHF.

1.3 Cardiac Resynchronization Therapy

1.3.1 Successes

CRT is a method by which the ventricles are paced with pacemaker leads to synchronize the ventricular contractions to each other and to the atria. There are devices that pace from the septal wall in the right ventricle or both ventricles, and there are devices that monitor the electrical activity of the heart to sense ventricular fibrillation and defibrillate when it is necessary. Typically, patients are paced biventricularly with leads at the RV apex and LV coronary sinus. Any of these methods have been shown to improve patients' quality of life and quantitative hemodynamic measures such as ejection fraction [5] [6] [7].

CRT also aims to correct the aggravating complication in which a person with chronic heart failure also has a conduction issue that culminates in an even lower ejection fraction. Preliminary studies looking at the effects of biventricular CRT on hemodynamic parameters were started in the 1990s. These studies showed that in patients with end-stage chronic heart

failure, who were denied or not eligible for heart transplants, biventricular pacing increased the mean cardiac index by 25%, decreased the mean V wave by 26%, and decreased the pulmonary capillary wedge pressure in a small study of eight patients [8]. Cardiac index is a measure of the cardiac output relative to the size of the individual, V wave is a measure of mitral valve regurgitation, and pulmonary capillary wedge pressure is an indirect measure of atrial pressure. This study by Cazeau et al. shows that biventricular pacing can improve the amount of blood that is distributed to the body while decreasing mitral valve regurgitation and decreasing atrial pressure [8]. They also showed that during follow-up studies the improvements were reversed when the pace making device was turned off [8]. The V wave observation that biventricular pacing decreased mitral regurgitation was confirmed in one of the patients via echo-Doppler evaluation [8]. The authors suspect that this is due to the pacemaker synchronizing mechanical activity of the mitral valve along with the electrical activity of the heart, perhaps with the papillary muscles [8]. Interestingly, the authors also found that one of the patients had a normal electrical activation sequence when he was paced with one lead of the pacemaker, but the activation sequence became abnormal when he was paced biventricularly. The abnormal activation seemed to be due to an ischemic injury in his ventricular septum [8]. This study was the first to look at the short-term effects of biventricular pacing on hemodynamic parameters, giving evidence that biventricular pacing could have a substantial, immediate effect on how the heart pumps to relieve some of the burden on a failing heart.

Evidence that suggests there is a significant improvement in certain hemodynamic parameters when a dyssynchronous, failing heart is paced biventricularly has been shown, but not that this increase in hemodynamic performance translates to improved performance in

clinical measures of cardiac function. Many papers, for example, the one by Auricchio et al demonstrate this [9]. They showed that in anaerobic and aerobic bicycle exercise, CRT leads to improved oxygen uptake [9]. The study optimized pacemaker placement and atrioventricular delay with respect to hemodynamic parameters and then looked at how pacing affected performance in peak exercise oxygen uptake, six-minute walk distance, quality of life score, and New York Heart Association (NYHA) functional class [9]. In all of these areas, patients improved significantly [9]. This study also investigated whether these clinical measures were significantly affected by the use of a single lead or biventricular lead. They found that optimal placement of a single lead (usually in the LV) could lead to similar increases in quality of life as biventricular leads [9].

Increases in hemodynamic function and increases in quality of life are important measures of how CRT can help patients, but another critical measure of how well this therapy works is how effective CRT is at keeping patients alive and out of the hospital. If CRT increases quality of life but increases the likelihood that the patients will die suddenly of heart related issues, it is not a very good method for treating chronic heart failure. However, a large scale randomized controlled trial suggests that CRT also decreases the likelihood that a patient will die and the likelihood that a patient will be hospitalized for heart or cardiovascular related events. The COMPANION study examined 1520 patients with advanced heart failure and long QRS interval [7]. The patients were NYHA class III or IV and had a QRS interval longer than 120 ms [7]. All patients received optimal pharmacological therapy such as diuretics, angiotensin converting enzyme inhibitors, and beta blockers, and were assigned to either a control group or a treatment group [7]. The treatment groups were either a pacemaker or a pacemaker-defibrillator, and the primary end point for the study was time to death from

any cause or hospitalization from any cause [7]. The COMPANION study found that both the pacemaker and the pacemaker-defibrillator groups experienced a decreased risk of hospitalization or death from any cause [7]. Also, the risk of hospitalization or death from heart failure was reduced by 34 and 40 percent for the pacemaker and pacemaker-defibrillator groups, respectively [7].

This COMPANION study is consistent with a meta-analysis of four randomized controlled trials of CRT. In a pooled analysis from the four trials, the authors found that death from progressive heart failure was reduced by 51 percent for patients who received CRT relative to controls [10]. The meta-analysis also found that CRT reduced hospitalization due to heart failure by 29 percent [10]. While the meta-analysis did not find a statistically significant difference in all-cause mortality, it did find a trend towards the reduction of all-cause mortality by CRT [10]. These analyses show that CRT improves patient outcomes with respect to death and hospitalization from heart failure while also improving short term hemodynamic function and patient quality of life.

1.3.2 Nonresponders

While CRT has a positive effect on outcomes for most patients, around 40 percent of people do not respond to CRT with reverse remodeling, and determining whether a patient responds is difficult [11]. A proposed predictor of the effectiveness of CRT is left ventricle dyssynchrony as measured with TDI. Defining a non-responder as someone who did not improve New York Heart Association class and did not see a 25 percent increase in the six-minute walk distance after pacemaker implantation, one can retroactively analyze the different factors that affected the outcome and determine what correlated best with the

response of patient. In one study, the dyssynchrony of the left ventricle showed the biggest difference between responders and non-responders, with responders having an intraventricular dyssynchrony of 87 ± 49 ms and nonresponders having an intraventricular dyssynchrony of 35 ± 20 ms [4]. Receiver-operating characteristic curve analysis showed that the optimal threshold led to a specificity and sensitivity of 80 percent at a threshold of 65 ms of left ventricle dyssynchrony [4]. These data also suggest that patients who receive a pacemaker with left ventricle dyssynchrony less than the threshold have an increased likelihood of adverse events such as cardiac death and hospitalizations for heart failure [4].

Another proposed method for identifying candidates for CRT is to measure the size of scar that a patient has due to myocardial infarction using delayed enhancement magnetic resonance imaging. Data suggest that patients with larger scar areas are more likely to be non-responders than those without, even if their left ventricle dyssynchrony is not significantly different [12]. In a relatively small study of 23 patients, a scar size threshold of 15 percent of the myocardium predicted with a sensitivity and specificity of 85 and 90 percent, respectively, whether a patient would respond to CRT [12]. A septal scar less than 40 percent of the septum had a sensitivity and specificity of 100 percent, and percent total scar correlated linearly with the response criteria [12].

More recently, a large-scale trial has suggested that of the many different ways to measure left ventricle dyssynchrony, none of them can be used to improve selection criteria for CRT. The PROSPECT trial was a large-scale trial with 53 centers in Europe, Hong Kong, and the United States that enrolled 498 patients with New York Heart Association class III or IV, left ventricular ejection fraction less than 35 percent, a QRS interval of greater than 130 ms, and optimal pharmacological treatment, and evaluated twelve echocardiographic

parameters of dyssynchrony [13]. The multi-center approach of a trial like the PROSPECT trial would ensure that any predictor of CRT is reproducible in many different centers and therefore a good predictor in general for recommending CRT. The PROSPECT trial was not able to recommend that any of the echocardiographic measures of dyssynchrony be used to predict outcomes of CRT [13].

1.3.3 Hyper-responders

While much time and energy has been spent investigating the subgroup of CRT patients classified as non-responders, a subgroup of patients called "hyper-responders" have been given much less attention. One reason this may be is that they make an almost complete return to normal cardiac function after CRT and therefore do not require any additional solutions. However, if this group could be well understood, then perhaps the mechanisms by which CRT does not work could be understood. In one study, the "hyper-responders" went from an ejection fraction of 25 ± 8 percent to an ejection fraction of 60 ± 6.5 percent after CRT [14]. The return to completely normal ejection fraction after CRT suggests that the dyssynchrony and the left bundle branch block were the primary causes of the chronic heart failure [14]. Interestingly, all the hyper-responders were from the group of patients with non-ischemic chronic heart failure [14]. This suggests that if researchers could accurately determine what effects an ischemic injury has on the conduction and contraction of the myocardium, then the outcomes of CRT could be accurately predicted.

1.4 Dyssynchrony Metrics

Many methods have been developed to distinguish between non-responders, responders, and hyper-responders. These techniques range from purely electrophysiological to mechanical in nature. Though all have them have demonstrated some ability to differentiate between the different groups, none have them have been proven to work consistently enough to be used to guide indications of CRT. This thesis will use some of these metrics calculated from finite elements simulations to predict response to CRT.

1.4.1 QRS Area

In one study of 57 patients, QRS area identified echocardiographic responders with a 10.2 odds ratio. This objective measure of patient electrophysiology performed at least as well as the most refined definition of LBBB [15]. QRS area is determined from the VCG and is defined as $(QRSx^2 + QRSy^2 + QRSz^2)^{1/2}$ where QRSx, QRSy, and QRSz are the time-integrated VCG in the x plane, y plane, and z plane, respectively [15]. The areas under the receiver operator characteristic curves were analyzed for several potential ECG and VCG metrics, and QRS area was had the largest area under the curve (AUC) of all of the metrics that were tested, beating QRS amplitude and QRS duration, as well as LBBB classifications [15]. QRS area may be clinically relevant because all patients will receive an ECG, so any metrics that could be directly derived from it could be used immediately by any hospital.

1.4.2 Circumferential Uniformity Ratio Estimate

The circumferential uniformity ratio estimate (CURE) is a metric derived from Fourier analysis of magnetic resonance- myocardial tagging (MR-MT) data [16]. It determines the

ratio of first- to zero-order power. A CURE of 0 represents pure dyssynchrony and a CURE of 1 represents complete synchrony. In control subjects, CURE indicated synchronous contraction even in patients where TDI indicated dyssynchrony [16]. CURE predicted improved NYHA function class with 90% accuracy [16]. CURE has since been used in a somewhat larger study of 75 patients, and it appears to be an accurate method for determining LV dyssynchrony and possibly differentiating between CRT responders and nonresponders, when the scar and delay of circumferential contraction at LV lead are taken into consideration using multivariate logistic modeling [17].

1.4.3 Internal Stretch Fraction

The internal stretch fraction (ISF) is a metric defined as the ratio of stretch to shortening during ejection [18]. This metric determines the amount of mechanical discoordination rather than mechanical dyssynchrony, because it does not look at the relative times that the stretches occur. Magnetic resonance with myocardial tagging (MR-MT) was used to calculate circumferential strain in the LV midwall, and the ISF was calculated by separating the strains that occur during ejection into stretching and shortening and finding the ratio between them [18]. In a study of 19 patients, the ISF was shown to be significantly higher in responders versus the nonresponders [18]. A difference between CURE and ISF is that the CURE assumes a sinusoidal spatial variation of strains, while the ISF does not.

1.4.4 Coefficient of Variation of Regional Work

The coefficient of variation of regional work (COVW) is a computational model-derived metric that represents the amount of heterogeneity in work throughout the

myocardium. The COVW is calculated from finite elements simulations by calculating the work from the stress and strain at each gauss point and dividing the standard deviation of the work by the mean of the work. Locations that are early activated tend to have low or negative work, because the strain and stress do not occur synchronously. When some areas are performing low or negative work, and others are performing high work, the COVW will increase. One paper showed that the COVW was sensitive to a LBBB activation pattern and may be a useful metric for determining dyssynchrony [19].

1.4.5 Volume Fraction of Negative Work

The volume fraction of negative work (VFNW) is another model-derived metric that represents the dyssynchrony of a contracting heart model. Negative work from this perspective means that the myofibers are lengthening during contraction instead of shortening. VFNW is calculated from finite elements simulations by calculating the work at each gauss point, then finding the volume associated with the gauss points that performed negative work and dividing by the total volume represented by the element or elements of interest. The VFNW may be calculated in certain areas of interest, such as the septum (VFSTNW) or the LV (VFLVNW).

1.5 Finite Element Models for Cardiac Electromechanical Simulations

Methods for developing finite element models for cardiac electromechanical simulations have been around for quite some time [20] [21] [22]. And in the last couple decades, finite element models with physiological circulatory models fully coupled to them been developed and made patient-specific [23] [24] [25] [26] [27]. The essential components

for these electro mechanical models are: cardiac geometry, an activation pattern, a constitutive model, an active model, and a circulatory model.

1.5.1 Cardiac Geometry

Before patient-specific geometries were readily available via computed tomography (CT) and magnetic resonance (MR), cardiac models were gross approximations that modeled the heart as a cylinder or a partial prolate spheroid [20] [21]. These models were able to provide general information about stresses and strains that were widely applicable, because the modeling error was greater than the patient-to-patient variability. Now, however, there are methods of making cardiac geometries that capture this variability and make patient-specific observations and predictions [26] [27].

1.5.1 Activation Pattern

Without a plausible activation pattern for these models, they could not capture the dyssynchrony of the patients. One method to create activation maps is to use computational models of electrophysiology with the patient-specific geometries to optimize the activation pattern to the clinically measured VCG [28].

1.5.2 Constitutive Models

The myocardium is a highly non-linear and anisotropic material, so the choice of constitutive model for the finite element simulation will be an important determining factor of the validity of the model. The myocardium is made of fibers that vary in direction based on their location. The fibers are arranged in sheets with other fibers that are in the same direction.

Because the myocardium is made of fibers and sheets, the mechanical properties are different in these directions. Models that consider the fiber direction but treat the sheet direction the same as the third direction, the sheet normal direction, are known as transversely isotropic constitutive models. Models that treat all three of the directions differently are known as orthotropic constitutive models.

Transversely isotropic models that have been proposed are typically simpler than the orthotropic counterparts, as they treat two directions the same. The first anisotropic model that considered the fiber structure was a sum of two exponential terms that had four material parameters [29]. Another empirical, transversely isotropic model is a five-parameter polynomial that had different values across the ventricular wall [30]. These models were developed when the myocardium was thought to be transversely isotropic, but the anisotropy in the cross-fiber directions has since been shown [31].

To capture the orthotropic nature of the myocardium, Fung-type exponential models with 7 or 12 material parameters were first developed [32] [33]. More recently, an orthotropic, convex constitutive model with parameters that are intuitively related to the underlying histology has been proposed [34].

1.5.3 Active Tension Models

Active tension models are needed to simulate the contractile forces inside the myocardium. The aforementioned fibers of the constitutive model are not passive materials but are made up of cardiomyocytes. Located inside of the cardiomyocytes are the contractile elements, known as sarcomeres. The proteins that make up sarcomeres slide along each other when activated by calcium transients. Some mathematical models of the myocardium model

the contraction of sarcomeres as an applied strain [35]. Physiologically, this is not accurate because the force increases in cardiac tissue whether the contraction is isometric, concentric, or eccentric. For this reason, models that use an active stress component added to the passive stress are more popular [36].

1.5.4 Circulatory Model

The best known and perhaps simplest circulatory models is the Windkessel model. It contains two components, an aortic compliance and a systemic resistance. The two-element Windkessel model does not provide accurate pressure waveforms with aortic flow as the input, so Windkessel models with three elements were developed [37]. While these models lead to accurate waveforms, the parameters did not closely correspond to physiological measurements. A fourth element was added to correct for this [38]. More parameters, for things like the baroreflex, blood volume regulation, and blood gas handling can be incorporated for a more integrated lumped parameter model, but the problem quickly becomes that there are too many parameters to fit each of them individually, especially for a patient-specific model. One solution to this problem uses physiological rules to find reasonable parameters for these processes without having to measure them directly, allowing patient-specific lumped parameter models with realistic physiology [39].

1.6 Specific Aims

CRT has proven to be an effective treatment for dyssynchronous heart failure in most patients with a long QRS duration, LBBB activation pattern, and an elevated ESV. CRT can improve quality of life, short-term heart function, and even lead to reverse modeling of the

ventricle to a more normal ESV. However, around 40% of patients that receive CRT do not respond [11]. Many metrics have been developed to try and separate the responders and non-responders so that only responders will receive CRT. None have proven to reproducibly separate patients in large, diverse cohorts. More recently, patient-specific electromechanical models have been used to model the diseased state, so the outcomes of CRT can be predicted. These models have not been validated thoroughly, and it is unclear how useful these models will be clinically, as they require invasive measurements.

To solve this problem, patient-specific models were developed from non-invasive clinical measurements. Average parameters from a previous cohort of patients were used wherever clinical measurements were unavailable. Metrics from the models were compared to models that contained invasive measurements. The sensitivity of the metrics to the parameters that went into the model was analyzed to determine what information is important to measure clinically. Knowing what the metrics are sensitive to will help us decide what clinical information should be included in these models and how closely the models need to match the clinical data.

Dyssynchrony metrics (ISF, CURE, COVW, VFNW) and their correlations with reverse remodeling as measured by change in ESV are compared between the two groups. The relative range of the metrics and predictive value of them are examined to determine if the models provide consistent results to their more patient-specific counterparts.

Circulatory model, active tension model, activation pattern, and geometry patient-specific parameters were each replaced with the average of the parameters from the patient group, to determine how important these parameters are to the aforementioned metrics.

Chapter 2 : Methods

Five electromechanical computational models were developed that captured patient-specific geometry, hemodynamics, and electrical activation. These models were compared with models that also included patient-specific mechanics and more hemodynamic information obtained via invasive measurements. The latter models were previously made [40]. The process by which the former were made is explained in this chapter. Meshes are generated from CT data, then electrical activation information is added, and hemodynamic parameters are estimated from echo data. Finally, heart beats are simulated until a steady state is reached and several metrics are calculated. This process is very similar to previous modeling work from the Cardiac Mechanics Research Group [26] [27].

2.1 Patient Data Collection

De-identified CT images and echocardiographic data were obtained from University of California, San Diego Healthcare System. Three male and two female patients with dilated cardiomyopathy (DCM), LBBB, and NYHA class II-III heart failure had all the necessary data at the necessary time points to be included in this study. Patient characteristics are summarized in Table 2.1.

Table 2.1: Summary of echocardiographic data retrieved prior to CRT device implant

Age	70 ± 7
EF	29 ± 5
LVEDV	167 ± 49
QRS Duration	156 ± 13

2.2 Mesh Generation

Patient CT scan data was segmented and exported via OsiriX. Separate segmentations were performed for the blood volume and myocardium. From these two segmentations, the epicardial and endocardial surfaces can be obtained. The segmentation data was imported into Blender, where it was smoothed and split into RV endocardial, LV endocardial, and epicardial surfaces. Subdivided icospheres were shrink-wrapped onto the smoothed surfaces to provide further smoothing. A 209-node template was fit to the shrink-wrapped objects such that the error from the segmentation and distortion of the faces were minimal.

The nodes were converted into prolate spheroidal coordinates, which are convenient for approximating the shape of the heart, by an algorithm that numerically estimates the value of μ and then calculates the values of ν and φ given the focal length, α. First, a guess of μ is initiated, then the y coordinate that would result from that μ, y_g, is calculated using Equation 1. Using the difference between, y and y_g, the μ is scaled until y_g is within a threshold of y. Then, the other values are calculated using Equation 2 and Equation 3.

$$y_g = \alpha \sinh(\mu) \sin\left(\arccos\frac{x}{\alpha \cosh(\mu)}\right) \cos \arcsin \frac{z}{\alpha \sinh(\mu) \sin\left(\arccos\frac{x}{\alpha \cosh(\mu)}\right)} \quad (1)$$

$$\nu = \mathrm{Re}\left(\arccos\frac{x}{\alpha \cosh \mu}\right) \quad (2)$$

$$\theta = \mathrm{Re}\left(\arcsin\frac{z}{\alpha \sinh \mu \sin \nu}\right) \quad (3)$$

The prolate spheroidal nodes were imported into Continuity, where the nodal coordinates were transformed into a tricubic Hermite finite elements mesh in cartesian coordinates. An example of what the stages of this process look like from segmentation to finite element mesh is given in Figure 2.1.

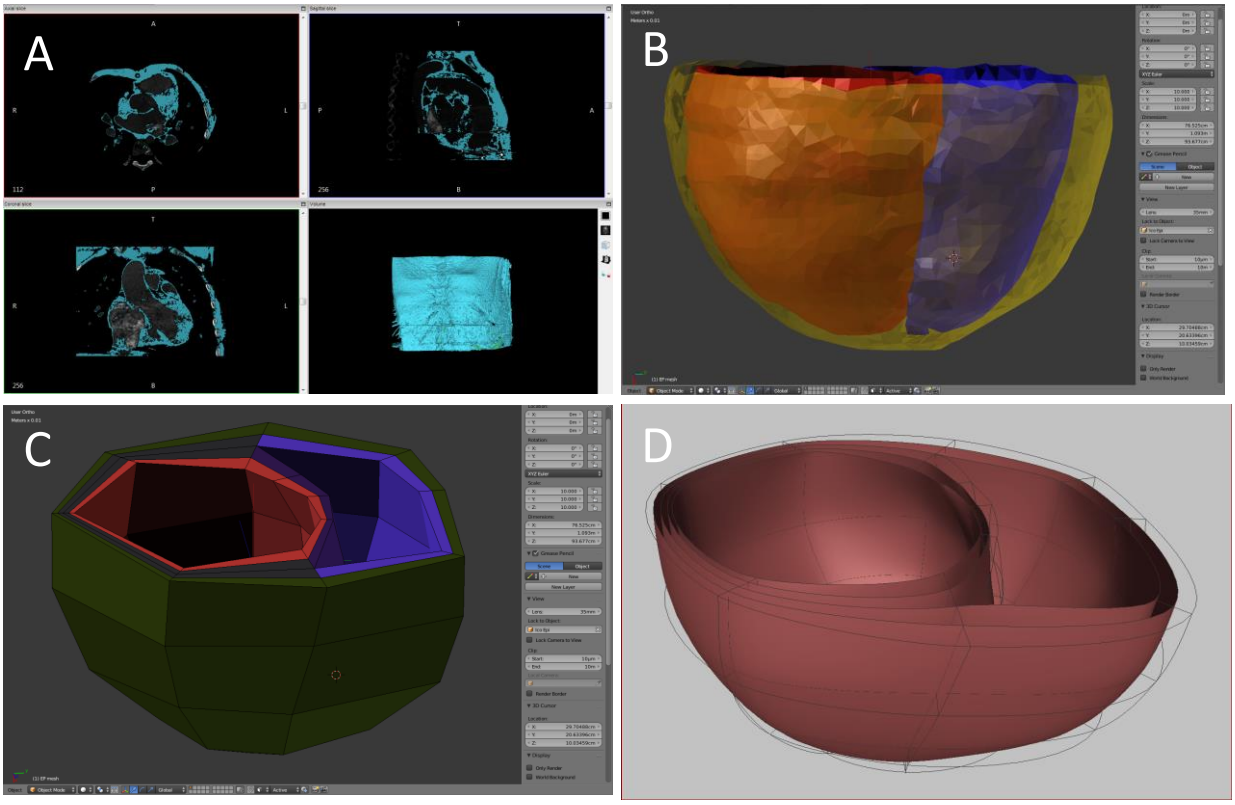

Figure 2.1: (A) Segmentation of CT imaging data. (B) Smoothed surfaces representing the LV endocardium (red) the RV endocardium (blue) and the epicardium (yellow). (C) 209-node template fit to the smoothed surfaces. (D) Finite element mesh after cubic splines were created in prolate spheroidal coordinates.

2.3 Fiber Fitting

The constitutive models discussed in 1.5.2 all have the stresses and strains with respect to the fibers of the tissue. In the current state, however, the models do not contain information about the direction of the fibers. To add fiber and sheet information, large deformation diffeomorphic mapping is used to map diffusion-tensor MRI data obtained from an isolated, fixed donor heart onto the finite element mesh. Fiber directions are shown in Figure 2.2.

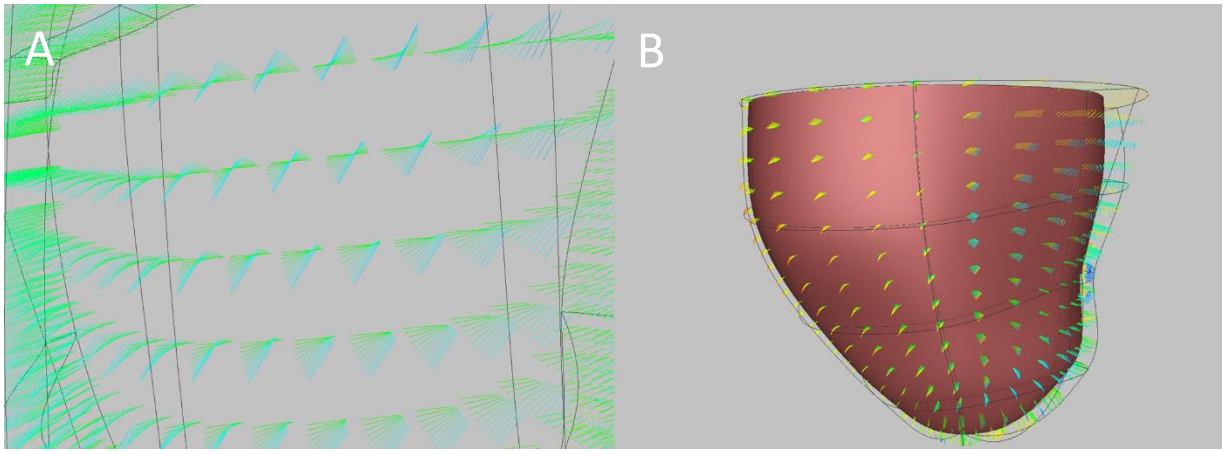

Figure 2.2: (A) Close up on an element, showing the transmural variation in fiber angle. (B) Showing spatial variation of fiber angle on the LV free wall.

2.4 Electrical Activation Maps

The electrical activation is what separates dyssynchronous heart failure from other types of heart failure. To ensure the models represented a dyssynchronous heart, patient-specific electrical activation maps were developed using the same methodology as the previously published models [28]. The finite element model developed previously was refined and exported back to Blender. A 280-node template was manually fit to the mesh-derived endo- and epicardial surfaces. HexBlender was used to calculate cubic derivatives and export the mesh back to Continuity, where the conductivity and stimulus location was adjusted to find the optimal combination to match the patient data. More specifically, the ECG was transformed to a VCG using the Kors method [41]. VCGs calculated from the finite element model were rotated into the same reference frame. The angular deviation between the Kors VCG was calculated and the simulation that had the least deviation was chosen. A mesh used in electrophysiological simulations and an example activation map are shown in Figure 2.3.

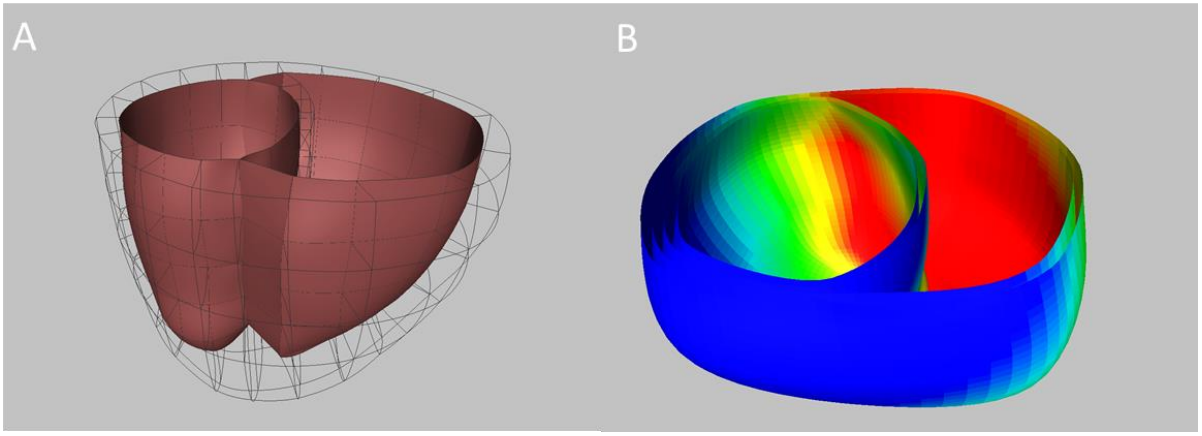

Figure 2.3: (A) An example electrophysiology finite elements mesh. This mesh would be subdivided for simulations. (B) An example of an LBBB activation map. Red is early activated, and blue is late activated.

2.5 Constitutive Model

The constitutive model used in these models is the Holzapfel and Ogden orthotropic model [34]. The model can be expressed in terms of the strain energy function shown in Equation 4, with the last term added to incorporate the slight compressibility of the myocardium. The invariant I_1 and quasi-invariants I_{4i} and I_{8fs} are defined in Equations 5, 6, and 7, respectively, where **C** is the right Cauchy-Green tensor, and $\boldsymbol{i_0}$ is the unit vector for the fiber, sheet, or sheet-normal direction.

$$\Psi = \frac{a}{2b} e^{b(I_1-3)} + \sum_{i=f,s} \frac{a_i}{2b_i}\left[e^{b_i(I_{4i}-1)^2} - 1\right] + \frac{a_{fs}}{2b_{fs}}\left[e^{b_{fs}I_{8fs}^2} - 1\right] + \frac{\kappa}{2}(det(\boldsymbol{F}) - 1)ln(det(\boldsymbol{F}))($$

$$I_1 = tr(\mathbf{C}) \quad (\mathbf{5})$$

$$\boldsymbol{I_{4i}} = \boldsymbol{i_0} \cdot (\mathbf{C}\boldsymbol{i_0}) \text{ for } \boldsymbol{i} = \boldsymbol{f}, \boldsymbol{s}, \boldsymbol{n} \quad (\mathbf{6})$$

$$I_{8fs} = \boldsymbol{f_0} \cdot (\boldsymbol{C}\boldsymbol{s_0}) \quad (7)$$

The material parameters: a, b, a_f, b_f, a_s, b_s, a_{fs}, and b_{fs} are positive material constants, where all "a" parameters have units of stress, and "b" parameters are dimensionless. The

subscripts: f, s, and n denote the fiber direction, sheet direction, and sheet normal direction, respectively. κ is the bulk modulus and $\boldsymbol{F}$ is the deformation gradient tensor. Values for each of these parameters were the average of the previous cohort [40].

2.6 Unloading Algorithm

With the patient-specific cardiac geometry, fiber orientation, and constitutive model in place, the unloading algorithm can be performed. The aim of the unloading algorithm is to obtain a plausible unloaded (zero-pressure) geometry for the heart. This is important for obtaining accurate values for stress during the full beat simulation. During the cardiac cycle, the heart is never at zero stress, and the unloaded state can only be truly found in an excised heart.

The algorithm works by inflating the end diastolic geometry to an end diastolic pressure (EDP). We did not know the patients' EDP, so we used the average of the previous cohort. The algorithm then calculates the deformation between the inflated geometry and the end diastolic geometry. The inverse of this deformation is applied to the starting geometry in a deflation step. The new deflated geometry is then inflated again. The inflation and deflation steps are repeated until the inflated geometry at EDP is sufficiently close to the measured end diastolic geometry. This process is the same as in the previous patients [26] [27] [40].

2.7 Active model

The active model is a Hill-type model, that uses two state variables: a contractile activation variable similar to calcium concentration in the sarcomere, and the length of the sarcomere. The sarcomere is modeled as a strain rate dependent element in parallel with a

contractile element and a strain dependent element in series. The rise and decay constants of the contractile element and a stress scaling factor for the peak tension development were adjusted to match the pressure tracings of the previous cohort. The average rise and decay constants were used in the new models, but the stress scaling factor was adjusted to match the clinical peak pressure data [36].

2.8 Circulation Model

The CircAdapt model was used, because physiological rules are used to find parameters that are not readily measurable clinically. Certain parameters, like the valve diameters, cardiac output, and mean arterial pressure, that are obtained by echocardiography were input into the model, and the model was allowed to adapt to give parameters that are consistent with the physiological rules that CircAdapt uses [39].

CircAdapt divides the circulatory system into modules: chambers, tubes, valves, and resistances. The atria and ventricles are modeled as chambers, where pressure depends on volume and sarcomere length. The major arteries and veins are modeled as tubes, where pressure only depends on volume. The capillary beds are modeled as resistances where the flow rate is a function of the pressure drop across them. There are six valve modules in the model, four for the actual valves in the heart, and two that represent the inertia of the blood at the entrance to the atria. The valves are flow ducts where the cross-sectional area depends on flow and transvalvular pressure [20].

Physiological rules for the tubes aim to maintain a consistent shear rate on the endothelium while keeping the wall stress under some maximum by changing the wall thickness and area. Chamber geometry is adjusted by changing the contractility and scaling

the wall volume accordingly. The pulmonary peripheral resistance is adapted to match the pressure drop across the lungs [20].

The CircAdapt model results in a set of ordinary differential equations (ODEs) That, when solved simultaneously, give accurate pressure wave forms and flows. The CircAdapt was first implemented in MATLAB, where many iterations of the model could be run in a relatively short time. The input parameters were adjusted such that the post-adaptation pressure-volume loops gave accurate peak pressure, EDP, and EF. The steady-state parameters for this model were then input into Continuity for the finite element full beat simulations' boundary conditions.

2.9 Full Beat Finite Elements Simulations

The end diastolic geometry, fiber information, activation map, constitutive model, unloaded geometry, active model, and circulation model were all combined in Continuity and run until the beats reached steady state. The finite elements simulation was solved to minimize cavity volume error using Newtonian iterations [23]. The EF and peak pressure were optimized to the measured values for our patients by adjusting the circulation model. The input parameters of the MATLAB CircAdapt model were scaled to adjust for errors between the heart model in CircAdapt and the finite element model.

2.10 Dyssynchrony Metrics

QRS area was calculated using the method outlined in section 1.4.1, from clinical ECG's for each patient. The CURE, ISF, VFSTNW, and VFLVNW were calculated from a script in MATLAB. Each was calculated according to the methods discussed in section 1.4.

Chapter 3 : Results

3.1 Model Comparison

The methods described above were used to generate five patient-specific models with mechanical properties and EDP that were the average of models where those data were known. The five patient-specific models developed for this thesis are called the "new models" or "new cohort," and the set of models from which the parameters were averaged is called the "previous models" or "previous cohort." The previous cohort followed similar methods but were developed with patient-specific mechanics that matched a pressure tracing from a ventricular catheter. Throughout the results section, these sets of models are compared to provide insight into what is important for calculating accurate patient-specific metrics of dyssynchrony.

3.1.1 Comparison with Patient Data

Though the model cohorts were built with different information, it will be useful to look at what clinical data was matched and how closely it was matched to discuss the validity of the models. The finite elements models were built from CT imaging and most of the rest of the patient data were obtained via echocardiography. To determine how consistent the echocardiographic and CT anatomies were, geometrical measurements similar to the ones obtained via echocardiography were gathered for the CT-derived meshes. These measurements include: interventricular septal thickness at diastole (IVSd), left ventricular internal dimension at diastole (LVIDd), and left ventricular posterior wall at diastole (LVPWd). Similarly, the QRS measured from the ECG is compared to that of the models. These data are shown in Figure 3.1.

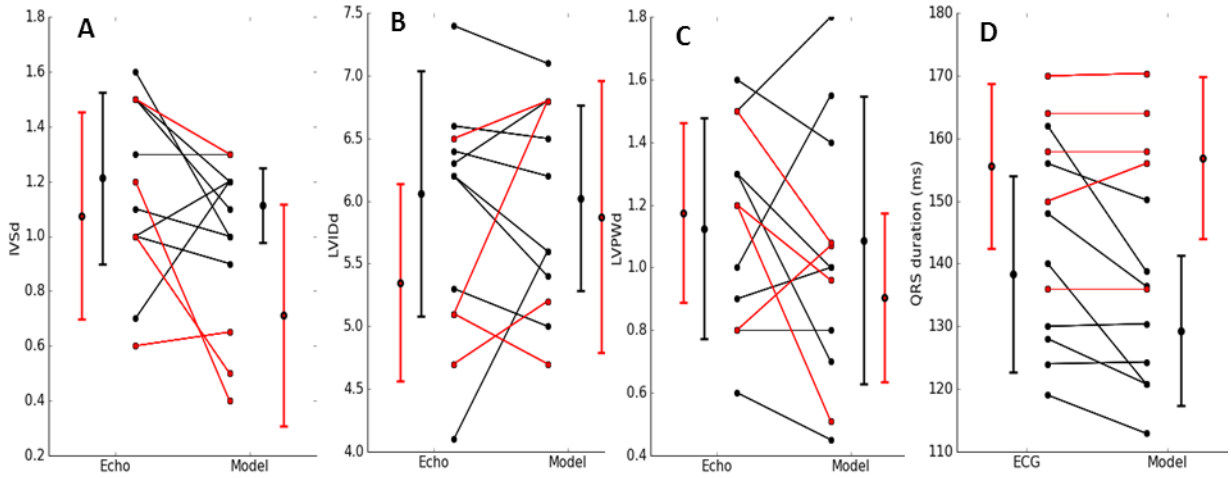

Figure 3.1: Comparing the two cohorts and the fitting of the data. The red is the new cohort and the black is the previous cohort. The lines connecting points from echo to model show the pairing of the data. The dots on the vertical lines are the mean, and the error bars are the standard deviation. (A) Comparison of the IVSd from clinical echo measurements and from the CT-derived model. (B) Comparison of LVIDd from echo and the CT-derived model. (C) LVPWd from echo and CT-derived model. (D) The QRS durations from the ECG and the model. Notice that the new cohort has, on average, longer QRS duration.

The activation maps were optimized to give a VCG that was as close as possible to the VCG constructed from the patient ECGs. The old cohort had a much more consistent activation pattern, with all of the patients' activation starting apically and close to the septum. The new cohort had activation patterns that ranged from apical and septal to more basal and towards the RV free wall. The activation maps are shown in Figure 3.2.

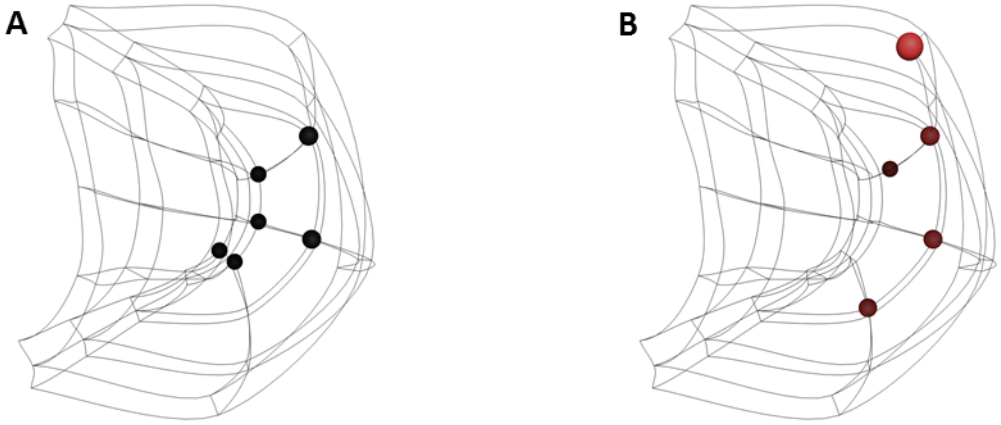

Figure 3.2: A view of the right ventricle of the model geometries. The outside is basal, and the middle is apical. (A) The earliest activated nodes for the previous cohort. There are fewer nodes than patients, because the same node was earliest activated for more than one patient. (B) The earliest activated nodes for the new cohort. Notice the larger variation in this cohort, with relatively more free-wall activation.

In the previous cohort, catheter pressures from the ventricles throughout cardiac cycle were available. Because of this, the mechanical properties were adjusted to match the - maximum and minimum pressure rates (dP/dt) in the ventricles and EDP. The new patients used the average mechanical properties and average EDP. Because of this, the new cohort had a much more consistent dP/dt. These data are summarized in Figure 3.3.

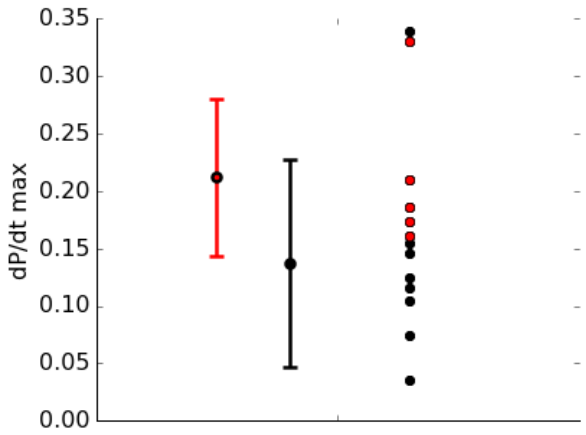

Figure 3.3: Comparison of dP/dt max from the previous cohort (black) and the new cohort (red). Notice the smaller range for the new cohort, because this was not fit to patient data. Instead, it correlates with the peak pressure.

Other hemodynamic data that were matched to clinical data are the EF, peak cuff pressure, and degree of mitral regurgitation. The mitral regurgitation was graded as trace, mild, moderate, and severe and was modeled by varying the lumen area of the mitral valve when its closed from 0.5% to 5% of its open area. The EF and peak pressure data are summarized in Figure 3.4.

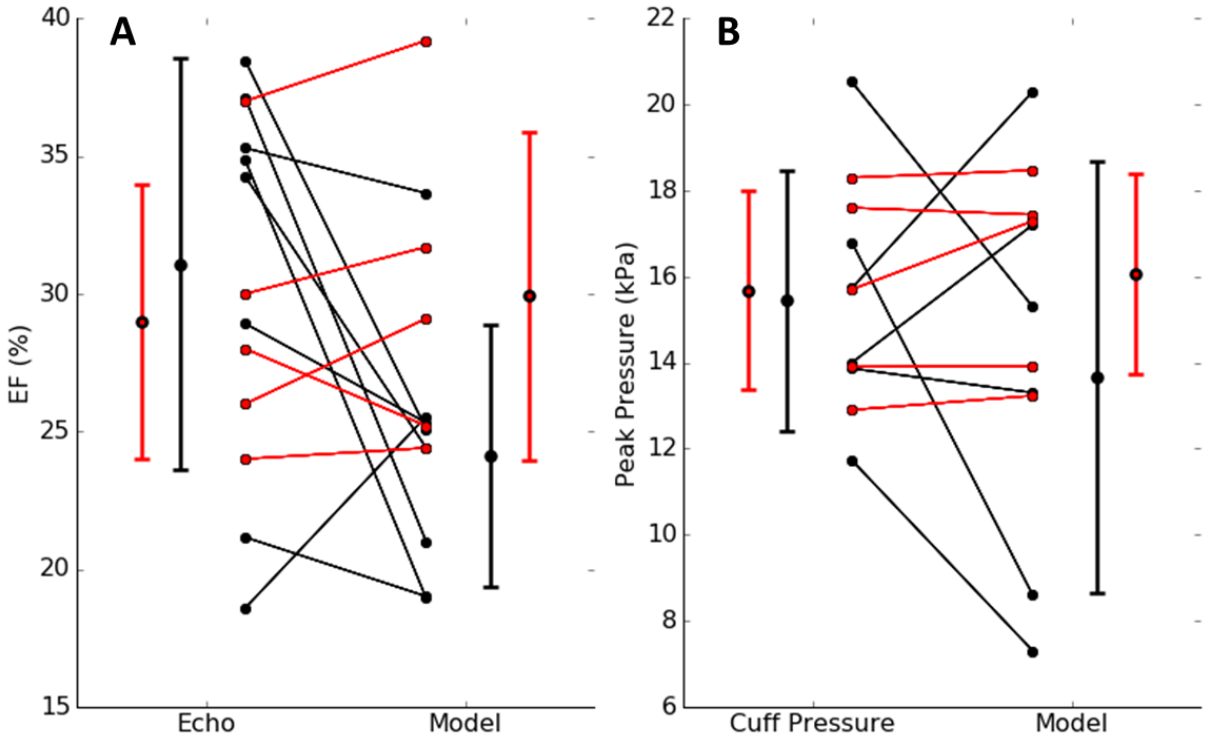

Figure 3.4: (A) The comparison of EF. Because the new cohort (red) was fit to the patient EF, it is much closer to the measured values. (B) The peak pressure was also fit in the new cohort instead of dP/dt max, so the models match the cuff peak pressure better.

3.1.2 Comparison of Metrics

The purpose for building these models is to determine which patients will respond to CRT and which patients will not. Typically, metrics of dyssynchrony are used, because a highly dyssynchronous heart theoretically has more opportunity to be made synchronous and therefore improve due to CRT. Many metrics have been developed in the literature, but the ones that will be focused on are VFLVNW, VFSTNW, COVW, CURE, and ISF. These metrics are discussed in detail in Chapter 1. Reverse remodeling as measured by a reduction in ESV is a common clinical endpoint for CRT response studies because reverse remodeling indicates that the pathologically dilated heart is remodeling to a more normal heart. The metrics will be used to predict reverse remodeling.

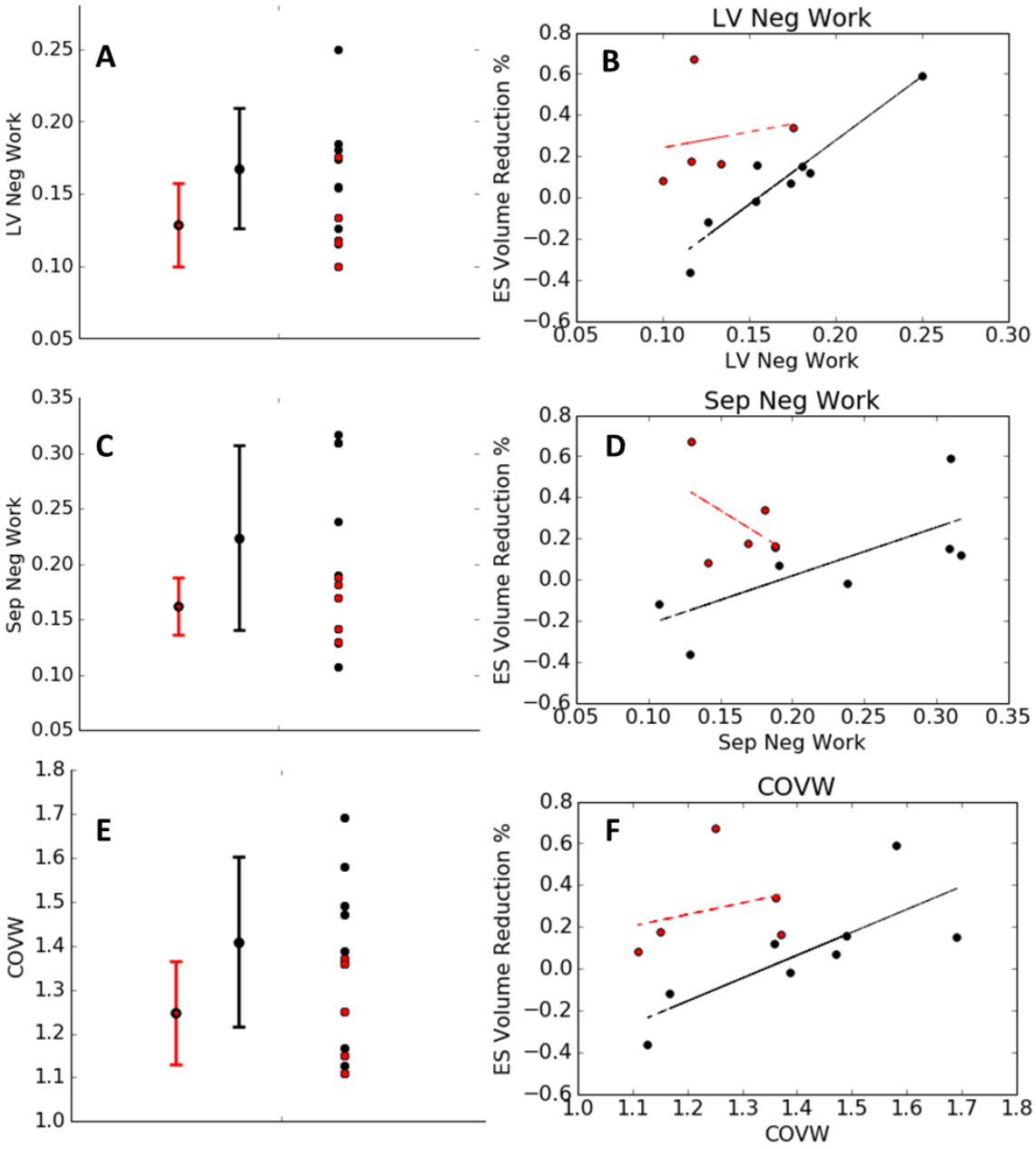

Figure 3.5: The left column shows the mean and variation of the metrics themselves. The right column shows the correlation with reverse remodeling. (A) New cohort (red) has less variation and is in general less dyssynchronous. (B) The VFLVNW vs. ESV reduction. A higher ESV reduction indicates a bigger response to CRT. The lines are linear regressions. Previously, the data had a strong correlation (r^2 = .9) that could separate responders from nonresponders. The correlation does not exist in the new cohort (r^2 = .03). (C) There is less variation and they are less dyssynchronous. (D) The modest correlation that existed in the previous cohort (r^2 = .5) is not there (r^2 = .2). (E) Again, the new models are more consistent and less dyssynchronous. (F) The correlation (r^2 = .6) is not existent in the new cohort (r^2 = .08).

3.2 Sensitivity Analysis

The previous models were built using the catheter pressures, such that the ventricular pressures throughout the cardiac cycle were known. The new models do not reproduce the same results although some variables, such as COVW and VFLVNW, showed similar trends. It is possible that the new models are accurately representing patient physiology, and the metrics are not useful for determining who will respond to CRT. It will be useful to determine what model parameters these metrics are sensitive to, so discussion of the validity of the models is well informed. For the sensitivity analysis, the previous models were used, so that the effect of average mechanical parameters could be investigated

3.2.1 Effects of Using Average Input Parameters

Several aspects of the previous models were made patient-specific, namely: the geometry, the activation pattern, the constitutive model, the dynamic model, and the circulation model. To see which of these model parameters affected the metrics, each one of them was changed to the average of the cohort while the others were left patient-specific and the metrics were recalculated. The normalized root mean squared deviation (nRMSD) from the fully patient-specific model to the models with one feature averaged was calculated, and the relationship between ESV reduction was investigated. The results are shown in Figure 3.6. The metrics were most sensitive to the average circulation model, and least sensitive to the average mechanics model.

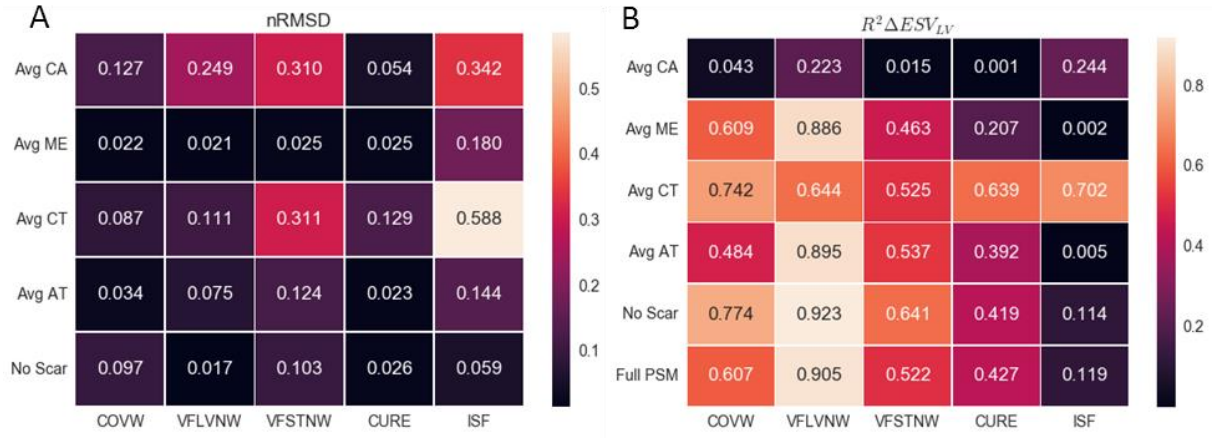

Figure 3.6: (A) Heatmap showing the nRMSD from the fully patient-specific model to the averaged parameter listed on the left. CA is the circulation model, ME is mechanical properties, CT is the geometry, and AT is the activation pattern. The bottom labels designate for which metric the nRMSD was calculated. Beige indicates a large change when the parameter was averaged, and purple indicates a small change. The average circulation and geometry had large effects on these metrics. (B) Heatmap showing the r^2 value between the metric at the bottom and the ESV reduction. The circulation model again had a large impact on all of the metrics except ISF, which did not originally show a correlation. The impact of averaging the geometry seems to be to increase these correlations, except in the VFLVNW.

3.2.2 Identification of Important Global Features

Identifying important clinical data to use to parameterize the models to give metrics that may be representative of patient CRT response can inform the collection of patient data for future studies. Features that are important for getting accurate work metrics will likely change when the metrics change and remain unchanged when the metrics do not change. Global, potentially clinically measurable features were calculated from the models. The features from patient-specific models were correlated with the same features from the models with average circulatory parameters, which changed the metrics the most. Also, they were correlated with the features from the models with average mechanical properties, which had the least effect on the metrics. The features that had little correlation in the average circulation model case and a strong correlation in the average mechanics case behaved similarly to the

metrics and are therefore likely important factors to match to clinical data, when possible. These features are RV and LV EDP, RV EDV, and LV maximum filling rate (dV/dt max). These data are summarized in Figure 3.7.

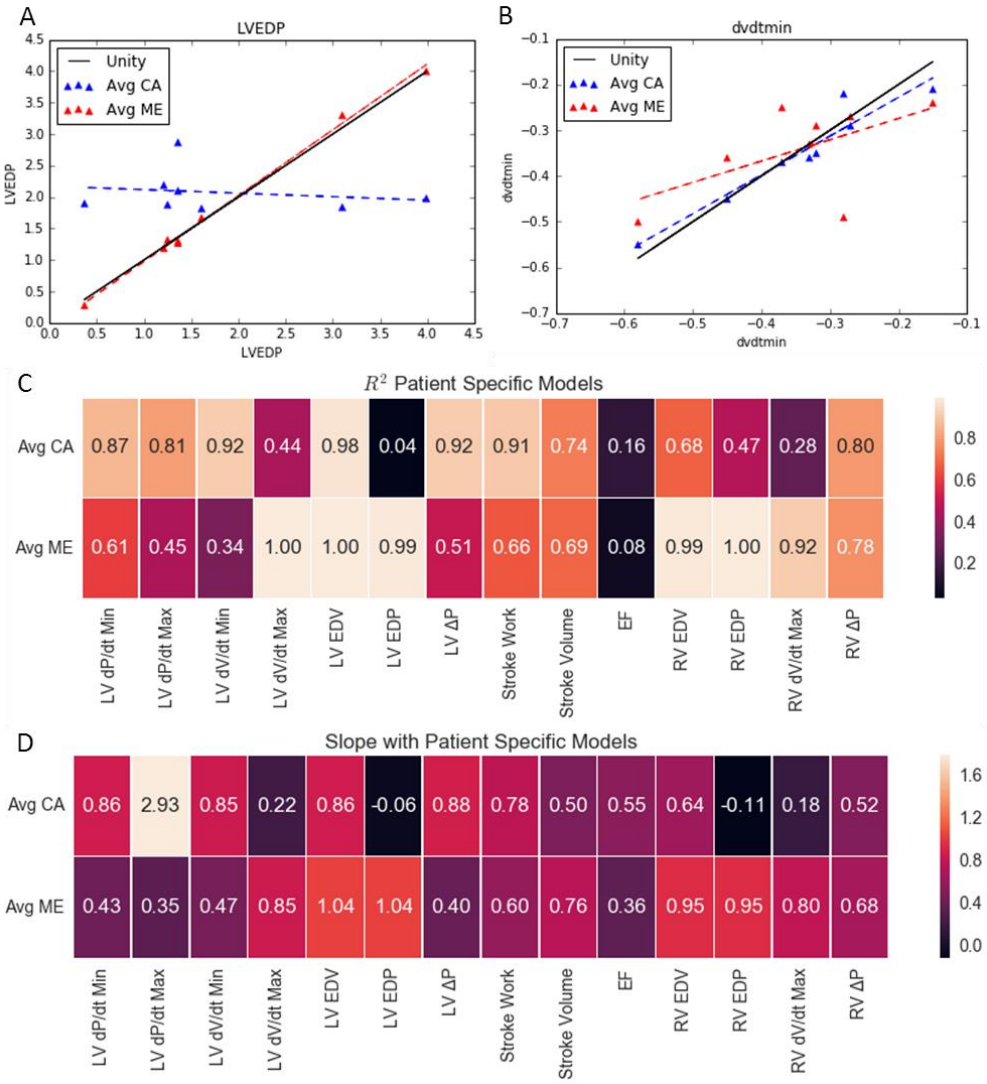

Figure 3.7: (A) The LVEDP from the fully patient-specific models plotted against the LVEDP from both the average circulation models and the average mechanics models. The line of best fit has the r^2 value and slope indicated in the heatmaps C and D. An r^2 value and slope of 1 indicates no change in the parameters. This example shows that the circulation model has a large effect and the mechanics has very little effect. (B) The ejection rate, dV/dt min is affected by mechanics more than the circulation model. (C) The r^2 values for the trendlines for each model are shown as a heatmap. (D) The slope of the trendline for each model.

The circulation model is crucial for calculating accurate dyssynchrony metrics. To determine which circulation parameters are related to the metrics, the residuals were correlated. The difference between each patient-specific parameter and the average of the parameter was plotted against the difference between the metrics under the fully patient-specific and average circulation model conditions. When the correlation is strong, it means that a change in that parameter is related to a change in the metric, and the more the parameter is changed, the more the metric is changed. This does not prove causation. The four parameters that correlated most strongly with each metric and how strongly they correlated are shown in Table 3.1. Most of them are related to ventricular preload and filling, and not as much the ventricular afterload.

Table 3.1: Results of correlating the residuals for the circulatory model. The four parameters that correlated best are shown. Notice how most have to do with ventricular filling via vein pressure or the atria.

VFLVNW		VFSTNW		COVW		ISF		CURE	
Parameter	r^2	Parameter	r^2	Parameter	r^2	Parameter	r^2	Parameter	r^2
Left atrial reference midwall area	0.79	Pulmonary veins reference pressure	0.66	Pulmonary veins reference pressure	0.74	Left atrial reference midwall area	0.87	Left atrial reference midwall area	0.68
Right atrial reference midwall area	0.77	Left atrial reference midwall area	0.66	Average LV short axis area	0.69	Right atrial reference midwall area	0.85	Right atrial reference midwall area	0.67
Pulmonary veins reference pressure	0.65	Average LV short axis area	0.64	Left atrial reference midwall area	0.62	Tricuspid valve lumen area when closed	0.78	Aorta unloaded lumen area	0.59
Average LV short axis area	0.64	Right atrial reference midwall area	0.63	Pulmonary artery reference pressure	0.62	Average LV short axis area	0.51	Tricuspid valve lumen area when closed	0.58

Chapter 4 : Discussion

4.1 Simulation Findings

In this thesis, five models with patient-specific geometries, activation patterns, EF, and peak pressure were developed. These models were compared to eight fully patient-specific models that also included patient-specific EDP, dP/dt, and mechanical properties. The new models were used to attempt to reproduce findings from the previous models, specifically that VFSTNW and VFLVNW are good metrics of dyssynchrony to predict reverse remodeling due to CRT. Also, a sensitivity analysis was performed to determine which inputs to the model are important for accurate dyssynchrony metrics. Patient-specific electromechanical models that do not contain patient-specific catheter pressure tracings are not able to reproduce the same predictive dyssynchrony indices as previous models. Sensitivity analysis suggests that while EDP is required, the full pressure tracing is not necessary to make accurate CRT predictive models.

The new models did not predict CRT response as well as the previous models, though they did display similar trends. The discrepancy may be because the two cohorts were different. The current group had longer QRS duration, because the guidelines for CRT were changed between the two cohorts. The activation patterns for these models were different in that they spanned a larger area of the RV and that they were on average more towards the RV free wall. Also, the previous models were matched to ventricular pressure tracings, while the new cohort only knew the peak pressure from a cuff blood pressure measurement. The dP/dt max has previously been identified as a potential predictor of response, though the sensitivity analysis suggests that it is not an important parameter for the dyssynchrony metrics [42]. The new models were consistently less heterogeneous by all the metrics that were calculated, and

the metrics spanned a smaller range. Either these patients had metrics that accurately represented their physiology and the metrics are not that useful for determining response to CRT, or the models did not capture the dyssynchrony present in the patients.

The sensitivity analysis suggests that the ventricular filling and EDP are important aspects to capture to ensure that the metrics that are calculated represent patient physiology. While this thesis has not shown a causal link between these aspects and the metrics, it has shown they are related. EDP was known for the previous models, but the average EDP of the previous cohort was assumed for the new patients. It is possible that not having this information is partially responsible for the relatively homogeneous models. The disadvantage of cardiac catheterization to get the pressure tracings is that it is an invasive procedure. There exist echocardiographic methods for estimating EDP, which could help make the metrics more representative of the patients, however these methods are better for estimating pressure *gradients* than absolute values [43] [44] [45] [46]. Also, ventricular filling via pulmonary pressures and atrial mechanics were found to be important. Pulmonary pressures can be estimated echocardiographically, though the accuracy of this method is debatable [47]. These somewhat inaccurate estimates may be better than not including this information at all as in the new models. Similarly, atrial mechanics can be estimated echocardiographically, but there are not clear standards or rigorous validation [48]. Because other pressure information like the dP/dt max and dP/dt min were not found to be important, a left heart catheterization may not be necessary. A right heart catheterization, which is much more routine but still invasive, may be able to provide enough information to make accurate models. The specificity of the metrics to EDP and ventricular filling mechanics in general should be studied first to determine

whether the invasive pressure tracing, invasive but routine EDP measurement, or the somewhat inaccurate echocardiographic estimates should be used in future models.

4.2 Limitations

The patient-specific geometries were segmented automatically using a threshold and the parts that are not needed are trimmed away manually. This is subject to user error, because sometimes the distinction between cardiac tissue and other surrounding tissues, such as hepatic tissue or the bone and muscle of the ribcage, is not clear. The choice of the valve plane is subjective, because the valves do not actually lie on the same plane. This could cause differences in the volume of the heart and shape of the heart near the base. A balance between fitting the data and good mesh quality also means that the patient-specific models can vary a little from the actual CT data. Finally, the highly detailed CT data is down sampled to just 209 nodes, and the elements are interpolated according to a prolate spheroidal assumption. This means that the geometries are approximations to the patient geometries rather than precise reconstructions of the geometries.

Many circulation model parameters are unknowns and are found by physiological rules in the CircAdapt program. The model is most sensitive to these parameters, so it is important that these parameters make sense with the patients' observed physiology.

These models take a very long time to develop. It took one year to develop these five, though the techniques are improving constantly. If these models are to be run to provide clinicians with information before patients are implanted, the workflow will need a major improvement and the computational runtime, currently 6 days for just the final simulation, will need to be much faster.

4.3 Future Studies

Though the patient groups in this thesis are not identical, the metrics used to evaluate dyssynchrony were not similar in the two groups. Perhaps the previous models should be created again in a blinded fashion using the same methods as the new models, and the metrics can be compared to see what effect knowing the invasive measurements had.

More needs to be known about the sensitivity of these models to the particular parameters that go into them. The circulation model, especially the EDP and ventricular filling mechanics should have its own sensitivity analysis performed. Then, whether the echocardiographic estimates or invasive but routine measurements of some of these parameters is good enough to provide reasonable accuracy for work metrics can be determined.

Because many patients do not receive cardiac CT, it can be difficult to build the patient-specific cardiac geometries. Because the average geometry did not worsen the correlation between metrics and ESV reduction, it may be possible to use an average geometry or scale an average geometry to fit the echocardiographic measurements of a patient. This may increase model throughput as well, because manual CT segmentation could be avoided.

REFERENCES

[1] S. Ghio, C. Constantin, C. Klersy, A. Serio, A. Fontana, C. Campana and L. Tavazzi, "Interventricular and intraventricular dyssynchrony are common in heart failure patients, regardless of QRS duration," *European Heart Journal,* p. 571–578, 2004.

[2] M. N. Levy and A. J. Pappano, Cardiovascular Physiology, 9th Edition., Philadelphia: Mosby, Inc., 2007.

[3] G. Ansalone, P. Giannantoni, R. Ricci, P. Trambaiolo, A. Laurenti, F. Fedele and M. Santini, "Doppler myocardial imaging in patients with heart failure receiving biventricular pacing treatment," *American Heart Journal,* vol. 142, no. 5, pp. 881-896, 2001.

[4] J. J. Bax, G. B. Bleeker and T. H. Marwick, "Left Ventricular Dyssynchrony Predicts Response and Prognosis After Cardiac Resynchronization Therapy," *Journal of the American College of Cardiology,* vol. 44, no. 9, pp. 1834-40, 2004.

[5] M. R. Bristow, L. A. Saxon, J. Boehmer, S. Krueger, D. A. Kass, T. D. Marco, P. Carson, L. DiCarlo, D. DeMets, B. G. White, D. W. DeVries and A. M. Feldman, "Cardiac-Resynchronization Therapy with or without Implantable Defibrillator in Advanced Chronic Heart Failure," *The New England Journal of Medicine,* vol. 350, no. 21, pp. 2140-2150, 2004.

[6] F. A. McAlister, J. Ezekowitz and N. Hooton, "Cardiac Resynchronization Therapy for Patients with Left Ventricular Systolic Dysfunction," *JAMA,* vol. 297, no. 22, pp. 2502-514, 2007.

[7] M. R. Bristow, A. M. Feldman and L. A. Saxon, "Heart failure management using implantable devices for ventricular resynchronization: Comparison of medical therapy, pacing, and defibrillation in chronic heart failure (COMPANION) trial," *Journal of Cardiac Failure,* vol. 6, no. 3, pp. 276-85, (2000).

[8] S. Cazeau, P. Ritter, A. Lazarus, D. Gras, H. Backdach, O. Mundler and J. Mugica, "Multisite Pacing for End-Stage Heart Failure: Early Experience," *Pacing And Clinical Electrophysiology,* vol. 19, no. 11, pp. 1748-1757, 1996.

[9] A. Auricchio, C. Stellbrink, S. Sack, M. Block, J. Vogt, P. Bakker, C. Huth, F. Schöndube, U. Wolfhard, D. Böcker, O. Krahnefeld and H. Kirkels, "Long-term clinical effect of hemodynamically optimized cardiac resynchronization therapy in patients with heart failure and ventricular conduction delay," *Journal of the American College of Cardiology,* vol. 39, no. 12, pp. 2026-33,

202.

[10] D. J. Bradley, E. A. Bradley, K. L. Baughman, R. D. Berger, H. Calkins, S. N. Goodman, D. A. Kass and N. R. Powe, "Cardiac Resynchronization and Death From Progressive Heart Failure: A Meta-analysis of Randomized Controlled Trials," *JAMA,* vol. 289, no. 6, pp. 730-40, 2003.

[11] P. W. Foley, F. Leyva and M. P. Frenneaux, "What is treatment success in cardiac resynchronization therapy," *Europace,* vol. 11, no. Suppl 5, pp. v58-v65, 2009.

[12] J. A. White, R. Yee, X. Yuan, A. Krahn, A. Skanes, M. Parker, G. Klein and M. Drangova, "Delayed Enhancement Magnetic Resonance Imaging Predicts Response to Cardiac Resynchronization Therapy in Patients with Intraventricular Dyssynchrony," *Journal of the American College of Cardiology,* vol. 48, no. 10, pp. 1935-60, 2006.

[13] E. S. Chung, A. R. Leon, L. Tavazzi, J.-P. Sun, P. Nihoyannopoulos, J. Merlino, W. T. Abraham, S. Ghio, C. Leclercq, J. J. Bax, C.-M. Yu, J. Gorcsan, M. St John Sutton, J. De Sutter and J. Murillo, "Results of the Predictors of Response to CRT (PROSPECT) Trial," *Circulation,* vol. 117, no. 20, pp. 2608-16, 2008.

[14] P. Castellant, M. Fatemi, V. Bertault-Valls, Y. Etienne and J.-J. Blanc, "Cardiac resynchronization therapy: "Nonresponders" and "hyperresponders"," *Heary Rhythm,* vol. 5, no. 2, pp. 193-7, 2008.

[15] C. J. M. van Deursen, K. Vernooy, E. Dudink, L. Bergfeldt, H. J. G. M. Crijns, F. W. Prinzen and L. Wecke, "Vectorcardiographic QRS area as a novel predictor of response to cardiac resynchronization therapy," *Journal of Electrocardiology,* vol. 48, no. 1, pp. 45-52, 2015.

[16] K. C. Bilchick, V. Dimaano, K. C. Wu, R. H. Helm, R. G. Weiss, J. A. Lima, R. D. Berger, G. F. Tomaselli, D. A. Bluemke, H. R. Halperin, T. Abraham, D. A. Kass and A. C. Lardo, "Cardiac Magnetic Resonance Assessment of Dyssynchrony and Myocardial Scar Predicts Function Class Improvement Following Cardiac Resynchronisation Therapy," *JACC: Cardiovascular Imaging,* vol. 1, no. 5, pp. 561-8, 2008.

[17] K. C. S. K. Bilchick, R. R. Yasmin S. Hamirani, S. A. Clarke, K. M. Parker, G. J. Stukenborg, P. Mason, J. R. M. John D. Ferguson, R. Malhotra, J. M. Mangrum and A. E. Darby, "Impact of Mechanical Activation, Scar, and Electrical Timing on Cardiac Resynchronization Therapy Response and Clinical Outcomes," *Journal of the American College of Cardiology,* vol. 63, no. 16, pp. 1657-66, 2014.

[18] B. Kirn, A. Jansen, F. Bracke, B. van Gelder, T. Arts and F. W. Prinzen, "Mechanical discoordination rather than dyssynchrony predicts reverse remodeling upon cardiac resynchronization," *American Journal of Physiology-Heart and Circulatory Physiology,* vol. 295,

no. 2, pp. H640-H646, 2008.

[19] R. C. Kerckhoffs, J. H. Omens, A. D. McCulloch and L. J. Mulligan, "Ventricular Dilation and Electrical Dyssynchrony Synergistically Increase Regional Mechanical Nonuniformity But Not Mechanincal Dyssynchrony," *Circulation: Heart Failure,* vol. 3, no. 4, pp. 528-36, 2010.

[20] T. Arts, P. C. Veenstra and R. S. Reneman, "Epicardial deformation and left ventricular wall mechanisms during ejection in the dog," *American Journal of Physiology-Heart and Circulatory Physiology,* vol. 243, no. 3, pp. H379-H390, 1982.

[21] P. H. M. Bovendeerd, T. Arts, J. M. Huyghe, D. H. v. Campen and R. S. Reneman, "Dependence of Local Left Ventricular Wall Mechanics on Myocardial Fiber Orientation: A Model Study," *Journal of Biomechanics,* vol. 25, no. 10, pp. 1129-40, 1992.

[22] T. P. Usyk, I. J. LeGrice and A. D. McCulloch, "Computational model of three-dimensional cardiac electromechanics," *Computing and Visualization in Science,* vol. 4, no. 4, pp. 249-57, 2002.

[23] R. C. P. Kerckhoffs, M. L. Neal, Q. Gu, J. B. Bassingthwaighte, J. H. Omens and A. D. McCulloch, "Coupling of a 3D Finite Element Model of Cardiac Ventricular Mechanics to Lumped Systems Models of the Systemic and Pulmonic Circulation," *Annals of Biomedical Engineering,* vol. 35, no. 1, pp. 1-18, 2007.

[24] R. C. P. Kerckhoffs, P. H. M. Bovendeerd, F. W. Prinzen, K. Smits and T. Arts, "Intra- and interventricular asynchrony of electromechanics in the ventricularly paced heart," *Journal of Engineering Mathematics,* vol. 47, no. 3-4, pp. 201-16, 2003.

[25] H. Watanabe, S. Sugiura, H. Kafuku and T. Hisada, "Multiphysics Simulation of Left Ventricular Filling Dynamics Using Fluid-Structure Interaction Finite Element Method," *Biophysical Journal,* vol. 87, no. 3, pp. 2074-85, 2004.

[26] A. Krishnamurthy, C. T. Villongco, J. Chuang, L. R. Frank, V. Nigam, E. Belezzuoli, P. Stark, D. E. Krummen, S. Narayan, J. H. Omens, A. D. McCulloch and R. C. Kerckhoffs, "Patient-specific models of cardiac biomechanics," *Journal of Computational Physics,* vol. 244, no. 1, pp. 4-21, 2013.

[27] J. Aguado-Sierra, A. Krishnamurthy, C. Villongco, J. Chuang, E. Howard, M. J. Gonzalez, J. Omens, D. E. Krummen, S. Narayan, R. C. P. Kerckhoffs and A. D. McCulloch, "Patient Specific modeling of dyssynchronous heart failure: A case study," *Progress in Biophysics and Molecular Biology,* vol. 107, no. 1, pp. 147-155, 2011.

[28] C. T. Villongco, D. E. Krummen, J. H. Omens and A. D. McCulloch, "Non-invasive, model-based measures of ventricular electrical dyssynchrony for predicting CRT outcomes," *EP Europace,* vol.

18, no. suppl_4, pp. iv104-12, 2016.

[29] J. D. Humphrey and F. C. P. Yin, "On Constitutive Relations and Finite Deformations of Passive Cardiac Tissue: I. A Pseudostrain-Energy Function," *Journal of Biomechanical Engineering,* vol. 109, no. 4, pp. 298-304, 1987.

[30] V. P. Novak, F. C. P. Yin and J. D. Humphrey, "Regional Mechanical Properties of Passive Myocardium," *Journal of Biomechanics,* vol. 27, no. 4, pp. 403-12, 1994.

[31] I. J. LeGrice, B. H. Smaill, L. Z. Chai, S. G. Edgar, J. B. Gavin and P. J. Hunter, "Laminar Structure of the Heart: Ventricular Myocyte Arrangement and Connective Tissue Architecture in the Dog," *American Journal of Physiology-Heart and Circulatory Physiology,* vol. 269, no. 2, pp. H571-82, 1995.

[32] K. D. Costa, J. W. Holmes and A. D. McCulloch, "Modelling Cardiac Mechanical Properties in Three Dimensions," *Philosophical Transactions of the Royal Society A Mathematical, Physical and Engineering Sciences,* vol. 359, no. 1783, pp. 1233-50, 2001.

[33] H. Schmid, M. P. Nash, A. A. Young and P. J. Hunter, "Myocardial Material Parameter Estimation - A Comparative Study for Simple Shear," *Journal of Biomechanical Engineering,* vol. 128, no. 5, pp. 742-50, 2006.

[34] G. A. Holzapfel and R. W. Ogden, "Constitutive Modelling of Passive Myocardium: a structurally based framework for material characterization," *Philosophical Transactions of the Royal Society A,* vol. 367, no. 1902, pp. 3445-75, 2009.

[35] S. Rossi, R. Ruiz-Baier, L. F. Pavarino and A. Quarteroni, "Orthotropic active strain models for the numerical simulation of cardiac biomechanics," *International Journal for Numerical Methods in Biomedical Engineering,* vol. 28, no. 6-7, pp. 761-88, 2012.

[36] J. Lumens, T. Delhaas, B. Kirn and T. Arts, "Three-Wall Segment (TriSeg) Model Describing Mechanics and Hemodynamics of Ventricular Interaction," *Annals of Biomedical Engineering,* vol. 37, no. 11, pp. 2234-55, 2009.

[37] N. Westerhof, G. Elzinga and P. Sipkema, "An artificial arterial system for pumping hearts," *Journal of Applied Physiology,* vol. 31, no. 5, pp. 776-81, 1971.

[38] N. Stergiopulos, B. E. Westerhof and N. Westerhof, "Total arterial inertance as the fourth element of the windekessel model," *American Journal of Physiology-Heart and Circulatory Physiology,* vol. 276, no. 1, pp. H81-8, 1999.

[39] T. Arts, T. Delhaas, P. Bovendeerd, X. Verbeek and F. W. Prinzen, "Adaptation to mechanical load determines shape and properties of heart and circulation: the CircAdapt model," *American Journal of Physiology-Heart and Circulatory Physiology,* vol. 288, no. 4, pp. H1943-54, 2005.

[40] A. Krishnamurthy, C. Villongco, M. Seidl, D. Krummen, S. Narayan, J. Omens, R. Kerckhoffs and A. McCulloch, "Abstract 11135: CRT Response is Greater in Patients With Larger Fraction of the Myocardium Performing Negative Regional Work," *Circulation,* vol. 128, no. Suppl 22, p. A11135, 2013.

[41] J. A. Kors, G. van Herpen, A. C. Sittig and J. H. van Bemmel, "Reconstruction of the Frank vectorcardiogram from standard electrocardiographic leads: diagnostic comparison of different methods," *European Heart Journal,* vol. 11, no. 12, pp. 1083-92, 1990.

[42] M. D. Bogaard, P. Houthuizen, F. A. Bracke, P. A. Doevendans, F. W. Prinzen, M. Meine and B. M. v. Gelder, "Baseline left ventricular dP/dt max rather than the acute improvement in dP/dt max predicts clinical outcome in patients with cardiac resynchronization therapy.," *European Journal of Heart Failure,* vol. 13, no. 10, pp. 1126-1132, 2014.

[43] K. S. Channer, P. Wilde, W. Culling and J. V. Jones, "Estimation of Left Ventricular End-Diastolic Pressure by Pulsed Doppler Ultrasound," *The Lancet,* vol. 327, no. 8488, pp. 1005-1007, 1986.

[44] S. Mulvagh, M. A. Quiñones, N. S. Kleiman, B. J. Cheirif and W. A. Zoghbi, "Estimation of Left Ventricular End-Diastolic Pressure fromDoppler Transmitral Flow Velocity in Cardiac Patients Independent of Systolic Performance," *Journal of the American College of Cardiology,* vol. 20, no. 1, pp. 112-9, 1992.

[45] S. R. Ommen, R. A. Nishimura, C. P. Appleton, F. A. Miller, J. K. Oh, M. M. Redfield and A. J. Tajik, "Clinical Utility of Doppler Echocardiography and Tissue Doppler Imaging in the Estimation of Left Ventricular Filling Pressures," *Circulation,* vol. 102, no. 15, pp. 1788-94, 2000.

[46] C. P. Appleton, J. M. Galloway, M. S. Gonzalez, M. Gaballa and M. A. Basnight, "Estimation of Left Ventricular Filling Pressures Using Two-Dimensional and Doppler Echocardiography in Adult Patients with Cardiac Disease," *Journal of the American College of Cardiology,* vol. 22, no. 7, pp. 1972-82, 1993.

[47] M. R. Fisher, P. R. Forfia, E. Chamera, T. Housten-Harris, H. C. Champion, R. E. Girgis, M. C. Corretti and P. M. Hossoun, "Accuracy of Doppler Echocardiography in the Hemodynamic Assessment of Pulmonary Hypertension," *American Journal of Respiratory and Critical Care Medicine,* vol. 179, no. 7, pp. 615-21, 2009.

[48] R. Leischik, H. Littwitz, B. Dworrak, P. Garg, M. Zhu, D. J. Sahn and M. Horlitz, "Echocardiographic Evaluation of Left Atrial Mechanics: Function, History, Novel Techniques, Advantages, and

Pitfalls," *BioMed Research International,* vol. 2015, no. 765921, pp. 1-12, 2015.

[49] B. W. L. De Boeck, A. J. Teske, M. Meine, G. E. Leenders, M. J. Cramer, F. W. Prinzen and P. A. Doevendans, "Septal rebound stretch reflects the functional substrate to cardiac resynchronization therapy and predicts volumetric and neurohormonal response," *European Journal of Heart Failure,* vol. 11, no. 9, pp. 863-71, 2009.